IJBPAS, June, 2021, 10(6): 1905-1923

ISSN: 2277–4998

International Journal of Biology, Pharmacy and Allied Sciences (IJBPAS)

'A Bridge Between Laboratory and Reader'

www.ijbpas.com

FABRICATION OF Fe_2O_3/W, N CODOPED ZnO BINARY COMPOSITES WITH EXCELLENT PHOTOCATALYTIC ACTIVITY AND PHOTOSTABILITY

E. KRISHNAN[1], M. RAVISHANKAR[*1] M. SIVAKUMAR[1&2] AND S. SIVAKUMAR[2]

1: Department of Chemistry, Rajah Serfoji Government College, Thanjur, Tamilnadu, INDIA

2: Department of Chemistry, E. R. K Arts and Science College, Dharmapuri, Tamilnadu, INDIA

***Corresponding Author: Dr. M.Ravishankar: E Mail: ravishankar1in@yahoo.co.in**

Received 13th July 2020; Revised 11th Aug. 2020; Accepted 20th Sept. 2020; Available online 1st June 2021

https://doi.org/10.31032/IJBPAS/2021/10.6.5515

ABSTRACT

Solar photocatalytic degradation of reactive azo dye such as reactive orange 30 (RO 30) using Fe_2O_3/W, N codoped ZnO were studied. A series of Fe_2O_3/W, N-codoped TiO_2 composites with different weight ratio (2 wt%, 4 wt%, 6 wt%, 8 wt%, and 10 wt%) were prepared dispersed method. The photocatalyst powders were characterized by X-ray diffraction (XRD), Scanning electron microscopy (SEM), UV–vis diffuse reflection spectroscopy (DRS) and Photoluminescence emission spectra (PL). Their solar photocatalytic activities were evaluated by the degradation of RO 30. The results generally show that the binary semiconductors Fe_2O_3/W, N codoped ZnO, with matching band potentials, exhibit better photocatalytic properties than the single phase Fe_2O_3, W, N codoped ZnO and ZnO. The effective electron–hole separation both at the chemically bonded interface and in the two semiconductors is believed to be mainly responsible for the increased photocatalytic performance of composites. The formation of chemically bonded interfaces between Fe_2O_3 and W, N codoped ZnO particles makes the interparticle charge transfer more spatially available and smoother, which is significant to enhance the photocatalytic activity. Reusability of the Fe_2O_3/W, N codoped ZnO powder in degradation of RO 30 was also possible as it gave a high consistent value of decolorization percentage (>90 %) even after the sixth repeated usage.

Keywords: Fe_2O_3/W, N codoped ZnO, surface morphology, sol-gel route, Photocatalytic Degradation, Reactive Orange 30 and Natural Sun Light

1. INTRODUCTION

A large number of dyes are produced annually, which is a basic requisite for various industries e.g., paper, textile, leather, cosmetic, food and pharmaceutical etc. There are approximately over 100,000 commercially accessible dyes with more than 70,000 t of annual production, 15% dye arelost in the process of dyeing **[1, 2]**. The occurrence of even small amount of dye in waste matter is noticeable and detrimental, which causes severe problem to human as well as aquatic life. Some azo dyes might undergo into possible cancer causing aryl amines in anaerobic circumstances. These problems have led to some new regulations relating to colored wastewater release as well as an obligatory use of more proficient effluent treatment techniques **[3, 4]**, versus conventional methods, which only transform the pollutants form one phase to another instead of mineralized and degrade in to harmless end products **[5-7]**.

In view of dyes contamination in water resources and degardation of environment **[8-12]**, efficient techniques are required to mitigate the dye contamination issue. Zinc oxide has been showed promising efficiency in advanced oxidation heterogeneous photocatalytic process due to its extraordinary characteristics like chemical and photo-stability. Using metal oxide based photocatalytic process, complete mineralization of toxic pollutants in wastewater can be achieved, which is one of major issue of environmental degradation **[13-19]**.

Solar photocatalysis in the presence of TiO_2, ZnO covers only the UV portion of the solar radiation. In order to enhance the photocatalytic activity, doping of ZnO with other metals and non-metal have been used. Doping of two kinds of atoms into wide band gap semiconductor oxides (ZnO or TiO2) has attracted considerable interest, since it could result in a higher photocatalytic activity and improved characteristics compared with single-element doping into semiconductor oxides. Co-dopants are generally classified as double nonmetal **[20, 21]**, metal–nonmetal **[22, 23]** and metal-metal **[24, 25]** elements. Several studies reported on codoped materials on ZnO with Pd and N, metallic silver and V.

The narrow-band-gap n-type α-Fe_2O_3 has also gained importance as a material for electronic, field-emission, electrochemical,

sensors, and lithium ion battery devices **[26-28]**. Hence, with the expect to achieve superior functionality and to integrate all of these different properties together in a single molecular structure. Many research works have focused on mixed oxide semiconductors due to an efficient charge separation can be obtained by coupling two semiconductor particles with different energy levels **[29-32]**. The improvement in efficiency of photocatalytic reactions is explained as result of a vectorial transfer of photogenerated electrons and holes from a semiconductor to another **[33, 34]**. ZnO has electronic properties and band gap energy similar toTiO_2 and it has been reported sometimes to be more efficient than TiO_2 for the photoxidation of phenol and nitrophenols **[35, 36]**. However, some combinations of ZnO with Fe_2O_3, TiO_2 or WO_3 have been investigated in order to enhance its photocatalytic activity on organic compounds photodegradation.

This paper describes Fe_2O_3/W N-doped ZnO composite powders were synthesized by polar solvent dispersed method. The powders were characterized by scanning electron microscopy (SEM), X-ray diffraction (XRD), ultraviolet-visible (UV-Vis) diffuse reflectance spectroscopy and photoluminescence study (PL). Photocatalytic degradation was used to evaluate on Reactive Orange 30 (RO 30).

2. MATERIALS AND METHODS

This work deals with the method of preparation of catalyst, characterization techniques and the experimental set-up used for the carrying out the photocatalytic degradation process.

2.1 Chemicals used

Reactive Orange 30 a widely used in textile dye with dichloroquinoxaline group and azo group supplied by Vexent dyeaux India Pvt. Ltd, Mumbai (Minimum dye content 70%) were used for photocatalytic degradation studies.

Chemical formula: $C_{29}H_{13}Cl_2N_5O_{13}S_4Na_4$

Molecular weight: 930.56

Water solubility: 70g/L at 293k

λ_{max}: 422 nm

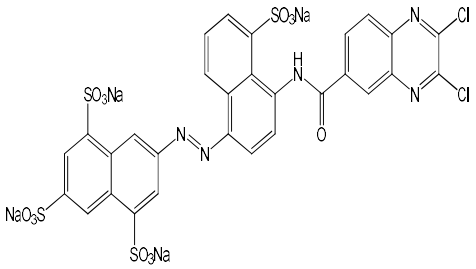

Figure 2.1: Structure of Reactive Orange 30

Zinc chloride (extra pure) (98%), Sodium tungstate (AR) Urea (AR), Sodium bicarbonate (99%) and Ferrous sulphate heptahydrate (GR) were supplied by Merck India Pvt. Ltd; dye solutions for photocatalytic studies were prepared in double distilled water. Sodium hydroxide and

hydrochloric acid (both AR grade from Qualigens) were used for modifying the pH of the solutions. Potassium dichromate (AR), Silver sulphate (GR), mercury sulphate (GR) 99% Ferroin (GR) and Sulphuric acid were used for COD analysis.

2.2 Preparation of W, N- codoped ZnO photocatalyst

In the preparation of W, N- codoped ZnO, 10 g of zinc chloride and 0.06 g of Sodium tungstate were dissolved in 100 ml of double distilled water. To that solution 6.2 g of sodium bicarbonate was then added in portions with vigorous stirring for several minutes. The precipitate formed was washed several times with distilled water to remove NaCl formed. Added 0.04 mol % of sodium tungstate and urea completely washed the precipitate to the suspension. The precipitate was then dried at 100ºC to remove the water. The solid obtained after drying was grinded in an agate mortar and pressed into a ceramic crucible. The material was calcinated at 500ºC for 4 hrs. The undoped ZnO was synthesised in the same procedure without adding dopant materials**.**

2.3 Synthesis of Fe_2O_3

In the preparation of Fe_2O_3, 10g of anhydrous Ferric chloride dissolved in 100 ml distilled water was converted into ferric hydroxide by slowly adding 1 M NaOH solution with vigorous stirring. Ferric hydroxide formed was washed with water and dried in hot air oven at 100°C to remove water and then solid obtained was grounded in a pestle mortar and calcinated at 500°C for 5 hours.

2.4 Preparation of Heterojunction Composite Photocatalysts

In the preparation of 2 wt % Fe_2O_3/W, N codoped ZnO heterojunction composites, 0.02 g of Fe_2O_3 was first dispersed in 40 ml of ethanol, to that suspension, 0.2750 g of oxalic acid was added, and the mixture was stirred in a magnetic stirrer to form a homogeneous suspension. To that suspension 0.98 g of W, N codoped ZnO was added, and the stirring was continued for 12 hours and then the suspension was dried and subsequently annealed at 300°C for 3 hours in a muffle furnace. The Fe_2O_3/W, N codoped ZnO heterojunction composites with 4, 6, 8 and 10 wt% of Fe_2O_3 were prepared by varying Fe_2O_3 and W, N codoped ZnO ratios as in a same method and labelled as FWZ-2, FWZ-4, FWZ-6, FWZ-8 and FWZ-10 respectively.

2.5 Photocatalytic degradation of Fe_2O_3/W, N codoped ZnO heterojunction composites

All the photocatalytic experiments were performed under natural sunlight on

clear sky days during the period of January to March-2019. In a typical experiment, 50 ml of dye solution (concentration 50 mg l^{-1}) was taken with 50 mg of photocatalyst in a 250 ml glass beaker. Then the dye solution was kept in direct sunlight with continuous aeration and the concentration of the dye remains was measured periodically by measuring its light absorbance at the visible λ_{max} by using Elico SL- 171 Visible spectrophotometer. In order to avoid the variation in results due to fluctuation in the intensity of the sunlight, a set of experiments have been carried out simultaneously. Oxidant combined photocatalytic degradation process were also done as mentioned method. For pH studies the pH of the dye solutions were modified to different values (3, 5, 7, 9 and 12) by using 0.1M HCl and NaOH solution.

2.6 Chemical Oxygen demand (COD)

For the analysis of COD, 0.4g of H_gSO_4 was added to 20 ml of the degraded dye solution in a 250 ml round bottom flask. To that 10ml of 0.25N $K_2Cr_2O_7$ was added and mixed well. Then 30 ml of H_2SO_4-$AgSO_4$ reagent (prepared by dissolving 0.5g of $AgSO_4$ in 30ml of Concentrated H_2SO_4) was added slowly with constant stirring. After that few pieces of pumice stones were added and the flask was fitted with a condenser and reflux for 2 hours. The solution was cooled and diluted to 150ml with distilled water and the entire content was titrated against 0.25 N Ferrous Ammonium Sulphate (FAS) solution using ferrion as indicator.

$$\textbf{COD in mg } l^{-1} = \frac{(V_1-V_2) \times N \times 8}{x}$$

Where V_1 & V_2 are the volume of FAS solution consumed for blank and test sample respectively, N is the normality of FAS solution and x is the volume of sample taken for analysis.

2.7 Characterization of Photocatalyst

X-ray powder diffraction (XRD) patterns of the photocatalysts were recorded on a Philips X'pert-MPD diffractometer in the 2h range 20°–80° using Cu Ka radiation. The data were collected with a step of 0.028 (2h) at room temperature. The phase structure of the products was determined by comparing the experimental X-ray powder patterns to the standard compiled by the Joint Committee on Powder Diffraction and Standards (JCPDS). The crystallite sizes were calculated from the peak width using the Scherrer equation. The surface morphologies and particle size were observed by Scanning Electron Microscopy (JEOL.JSM-6360LV). UV-visible diffuse reflectance spectra were acquired by a

Perkin-Elmer Lambda 35 spectrometer. BaSO4 was used as the reflectance standard.

3. RESULT AND DISCUSSION

3.1 Physicochemical characterization of the photocatalyst

3.1.1 X-ray diffraction studies

The powder XRD patterns of ZnO, Fe_2O_3 and Fe_2O_3/W,N codoped ZnO were as shown in **Figure 3.2.** The ZnO samples were identified by XRD as a single phase containing wurtzite crystalline structure (JCPDS card nos.: 89-1397; 89-0511; 36-1451). The high intensity of the peaks indicates that ZnO are of high crystallinity **[37]**. The crystalline structure of Fe_2O_3 also be exactly matches corresponding original standard card values. The absence of diffraction peaks corresponding to FeO or Fe_3O_4 in the XRD patterns of Fe_2O_3/ZnO indicates the uniform dispersion of Fe_2O_3 ions. Moreover the bulk structure remains virtually unchanged by the Fe_2O_3 coatimg. The Fe_2O_3 concentration increases on W,N codoped ZnO, th1e crystalline phase decreased. The reason is low crystalline Fe2O3 could be covered on W,N ZnO.

3.1.2 SEM analysis of the photocatalysts

Figure 3.3 demonstrate the SEM images of pure ZnO, pure Fe_2O_3, W,N codoped ZnO and different weight ratio of Fe_2O_3 coated W,N codoped ZnO composites. SEM image of pure ZnO shown in **Figure 3.3** a providing visualization of the textural properties of small portions of aggregated particle indicates that the pure ZnO is made up of irregularly shaped aggregates. Pure Fe_2O_3 SEM image (**Figure 3.3 b**) shows small particles dispersed with agglomerated surface. **Figure 3.3 c** indicates the micrographs show that W,N codoped ZnO have blunder particle morphology. Addition of Fe_2O_3 has significant effect on the small particle morphology and further increases the level of Fe_2O_3 concentration (**Figure 3.3 d and e**) the particle upto 8wt% the particles highly dispersed and small particle size and particularly this weight ratio (8wt%) composites shows needle like structure. It is presumed that the concentration of Fe_2O_3 as a coupling precursor played a key role in the formation of the peculiar morphology of spheres. After the decoration of Fe_2O_3 particles, the spongy materials are observed on the surface of W,N codoped ZnO (**Figure 3.3 f**). From this study 8 wt% Fe_2O_3/W,N codoped ZnO birnary composite has suitable for solar light photocatalytic degradation.

3.1.3 Diffused Reflectance UV-Visible analysis of the photocatalyst

Diffused reflectance spectra UV-visible spectra of ZnO, W,N codoped ZnO and various weight ratio of Fe_2O_3/W,N

codoped ZnO were given in **Figure 3.4.** The results show that the absorption onset of ZnO, W, N codoped ZnO and Fe_2O_3/W,N codoped ZnO were 390, 420 and 600 nm respectively. Therefore Fe_2O_3/W,N codoped ZnO can utilize more visible light than the W, N codoped ZnO and pure ZnO for photoexcitation process and expected to have more activity in the solar radiation than the W, N codoped ZnO and pure ZnO. The reason of red shift in the light absorption of W,N codoped ZnO due to coating of Fe_2O_3.

3.1.4 Photoluminescence study

To exhibit the proposed photocatalytic mechanism, we have measured the photoluminescence behavior of the photocatalyst system. Photoluminescence has been widely employed in the field of photocatalysis over solid semiconductor as a useful probe for understanding the efficiency of charge-carrier trapping, immigration and transfer, and to understand the recombination processes of photogenerated electron (e-)–hole (h+) pairs **[34]**. **Figure 3.5** shows the photoluminescence (PL) emission spectra of pure ZnO W,N codoped ZnO and Fe_2O_3 coated W, N-codoped ZnO composite photocatalyst. ZnO has a peak at 600 nm in the PL spectrum which corresponds to the recombination of the electron (e^-) and hole (h^+) formed. The emission is significantly weakened or disappears completely in the Fe_2O_3 coated W, N-codoped ZnO composites.

The observable lower PL intensity at 600 nm implies that the recombination of charge-carriers is effectively inhibited, which probably leads to a higher photocatalytic activity since the photodegradation reactions are induced by these carriers **[35]**. This result demonstrates good agreement with the proposed mechanism of efficient separation of charge-carriers, as discussed above.

3.2 Photocatalytic studies

3.2.1 Photocatalytic degradation of Reactive Orange 30

Photocatalysis has become one of the most gifted technologies due to its potential applications in solar energy conversion to solve the worldwide energy scarcity and environmental pollution. As is well known, solar light is an unlimited supply of energy in nature. There is only a small portion (4%) of solar radiation in the UV region, while visible light is far more abundant (> 46%), thus enhancing the photocatalytic capability of semiconductors under visible light as well as UV light irradiation has become an necessary issue in order to highly utilize solar energy. To study the photocatalytic degradation efficiency of the Fe_2O_3/ W,N codoped ZnO photocatalytic system, the

photocatalytic activities of various photocatalysts materials are evaluated for the degradation of RO 30 solution as a model dye effluent under irradiation with solar light. Dark adsorption of dye molecules is measured for 20 min to reach an adsorption-desorption equilibrium. In this work, RO 30, with a characteristic absorption at 430 nm, is chosen as a typical dye pollutant for testing the photocatalytic activity of the as-prepared products under both UV and visible light irradiation. **Figure 3.6 (a)** shows the instantaneous RO 30 concentrations variations versus time in the presence of Fe_2O_3/ W,N codoped ZnO composites, as well as parent photocatalyst under solar light irradiation, respectively. The graphs in the first 20 min before light irradiation are caused by the RO 30 adsorption-desorption process on the catalyst surfaces. It can be seen that only 4% decrease in the concentration of RO 30 can be observed in the presence of ZnO as the adsorption-desorption equilibrium of RO 30 on the surface of ZnO photocatalyst reaches in dark after 20 min. Whereas, the adsorption ability of RO 30 over Fe_2O_3, ZnO, W,N codoped ZnO and Fe_2O_3/ W,N codoped ZnO composite system is up to increase 20% respectively, which may be attributed to the smaller particle size with high specific surface area.

The optimized W,N codoped ZnO heterojunction semiconductor was further tested the photocatalytic degradation ability when modified with various concentration of Fe_2O_3 with W,N codoped ZnO under the solar light irradiation. After 60 min of solar light illumination, the RO 30 degrades over Fe_2O_3, W,N codoped ZnO and Fe_2O_3/ W,N codoped ZnO composite are only 15%, 25%, 40% and 70%, respectively. However, Fe_2O_3/W,N codoped ZnO composite semiconductors shows higher photocatalytic degradation rate(80–98%) in the presence of same experimental conditions. It is worth noting that Fe_2O_3 coated W,N codoped ZnO semiconductor could be inducing notable photodegradation efficiency from 80% to 98% beyond the increases of 8 wt % of Fe_2O_3.

From the results, the photocatalytic activity of W,N codoped ZnO systems increases with the increase in Fe_2O_3 content 2 wt% to 8 wt % due to the tightly bonded or close contact interfaces between Fe_2O_3 and W,N codoped ZnO, by which the injection of photogenerated electron of Fe_2O_3 transfer of conduction band of W,N codoped ZnO and also absorbs visible light. On the contrary, when the mass ratio was higher than 8 wt%,

the Fe_2O_3 got agglomerated and it was not well dispersed. This hinders the smooth contact between W,N codoped ZnO systems and Fe_2O_3, leading to a negative influence on the activity of the 10 wt % Fe_2O_3 coated W,N codoped ZnO semiconductor composite. The studies also show that photoelectron injector such as Fe_2O_3 has very low photocatalytic activity in UV-visible light when compared to that of W,N codoped ZnO and ZnO photocatalysts. This shows that the Fe_2O_3 has a smaller electron-hole diffusion length than the W,N codoped ZnO and ZnO photocatalysts.

The kinetics of degradation of RO 30 over ZnO, W,N codoped ZnO and Fe_2O_3 coated W,N codoped ZnO composite has been studied in natural sunlight. The normalized C/C_0 Vs time plots for the dyes were given in **Figure 3.6b.** The data were also analysed with the Langmuir–Hinshelwood kinetic model:

$$r = \left(\frac{kKC}{1 + KC} \right)$$

Where r is the specific degradation reaction rate the dye ($mgl^{-1}min^{-1}$), C the concentration of the dye (mg l^{-1}), k the reaction rate constant (s^{-1}) and K is the dye adsorption constant. When the concentration (C) is small enough, the above equation can be simplified in an apparent first-order equation **[37]**:

$$\left(-\frac{dC}{dt} \right) = r = kKC = k_{app}C$$

After integration, we will get

$$-\ln\left(\frac{C}{C_0} \right) = k_{app}\, t$$

Where C_0 is the initial concentration (mg l^{-1}), C is the concentration of the dye after t minutes of illumination and k_{app} is the apparent first order rate constant. The plots obtained were shown as **Figure 3.6 b.** The photocatalytic degradation of RO 30 on Fe_2O_3/W,N codoped ZnO was found to be faster than that of the pure ZnO and W,N codoped ZnO. The Fe_2O_3/ W,N codoped ZnO shows higher activity than the W,N codoped ZnO and pure ZnO, the reason is due its band gap difference **[38]**.

3.2.2 Effect of pH of the dye solution on Fe_2O_3/W,N codoped ZnO

The influence of initial pH of the dye solution on degradation efficiency of Fe_2O_3/W,N codoped ZnO composite was shown in **Figure 3.7.** The photocatalytic degradation of the RO 30 reaches the maximum, when pH of the dye solution was pH 5. The point of zero charge of ZnO was pH 9 **[39]**. Therefore its surface becomes positively charged when the pH of the solution was below 9 and the density of positive charge in the surface of ZnO increases with the decrease of pH value. Due

to the anionic nature of the RO 30, its adsorption on positively charged Fe_2O_3/W,N codoped ZnO surface was very high. The photogenerated holes easily oxidise dye molecule when dye molecules are adsorbed on the photocatalyst surface of the photocatalyst. Hence the rate of degradation of RO 30 was maximum at pH 5.

3.2.3 Chemical Oxygen Demand (COD) analysis

The Chemical oxygen Demand test is widely used as an effective technique to measure the organic load in the wastewater and also to estimate the degree of mineralization of organic pollutant in water treatment. The analysis measure the organic load present in the water in terms of the total quantity of oxygen required to oxidize them to CO_2 and water**.** The reduction in COD values of the RO 30 solution before and after the treatment was estimated. **Table 3.1** gives the percentage of degradation of dye calculated from spectrophotometric data and COD values for ZnO and Fe_2O_3/W,N codoped ZnO. The reduction in COD values of the treated dye solution indicates that the dye solution was not only decolourised but also mineralized into smaller molecules like CO_2**,** NO_2 and so on**.** The mineralisation of RO 30 has lower percentage than the degradation; it might be due to the presence of dichloroquinoxaline group and azo group, which are reported chemically more stable than phenyl groups **[40]**.

3.2.4 Reusability Test

To assess the stability of the photocatalyst on reuse, the same Fe_2O_3/ W,N codoped ZnO composites was used in consecutive photocatalytic experiments for the degradation of RO 30 up to five cycles. The degradation of the 50 mg/l RO 30 dye solution at pH 3 over fresh Fe_2O_3/ W,N codoped ZnO composites was 100 % in 2 h of sunlight irradiation. After the first cycle, the photocatalyst was separated from the dye solution and added to 50 ml of fresh dye solution for the next experimental cycle. On the reuse, the percentage of degradation of dye observed was 100, 99 and 96 in the first, second and third cycle respectively (**Figure 3.8**).

The slight decrease in the activity of the photocatalyst after each cycle may be due to the residual intermediates of the degraded dye adsorbed on surface of photocatalyst **[41]**. The results show that the reused Fe_2O_3/ W,N codoped ZnO has about 96 % of the activity of fresh catalyst in its third cycle. Hence, it will be a good material for the degrading the organic dyes in textile effluents.

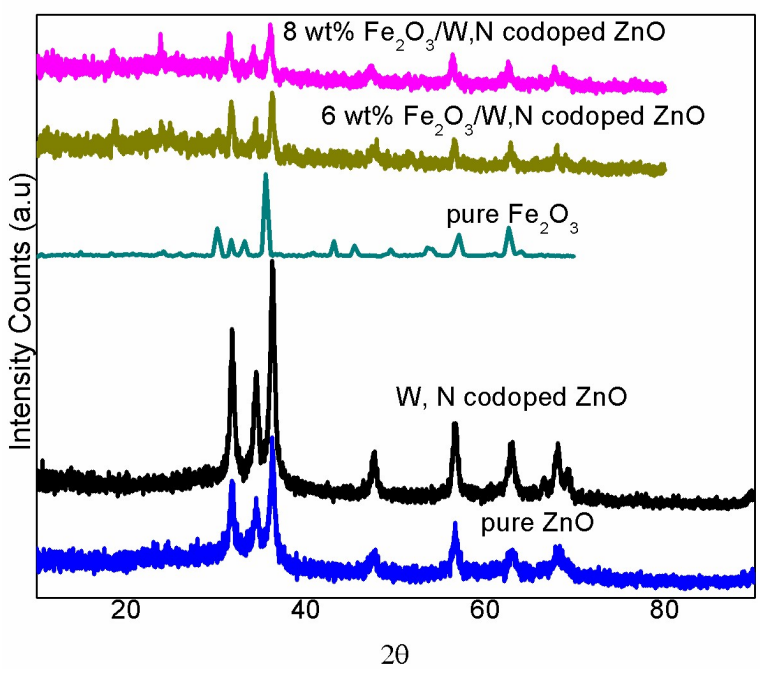

Figure 3.2 XRD patterns of Fe_2O_3, ZnO, W,N codoped ZnO and Fe_2O_3/ W,N codoped ZnO

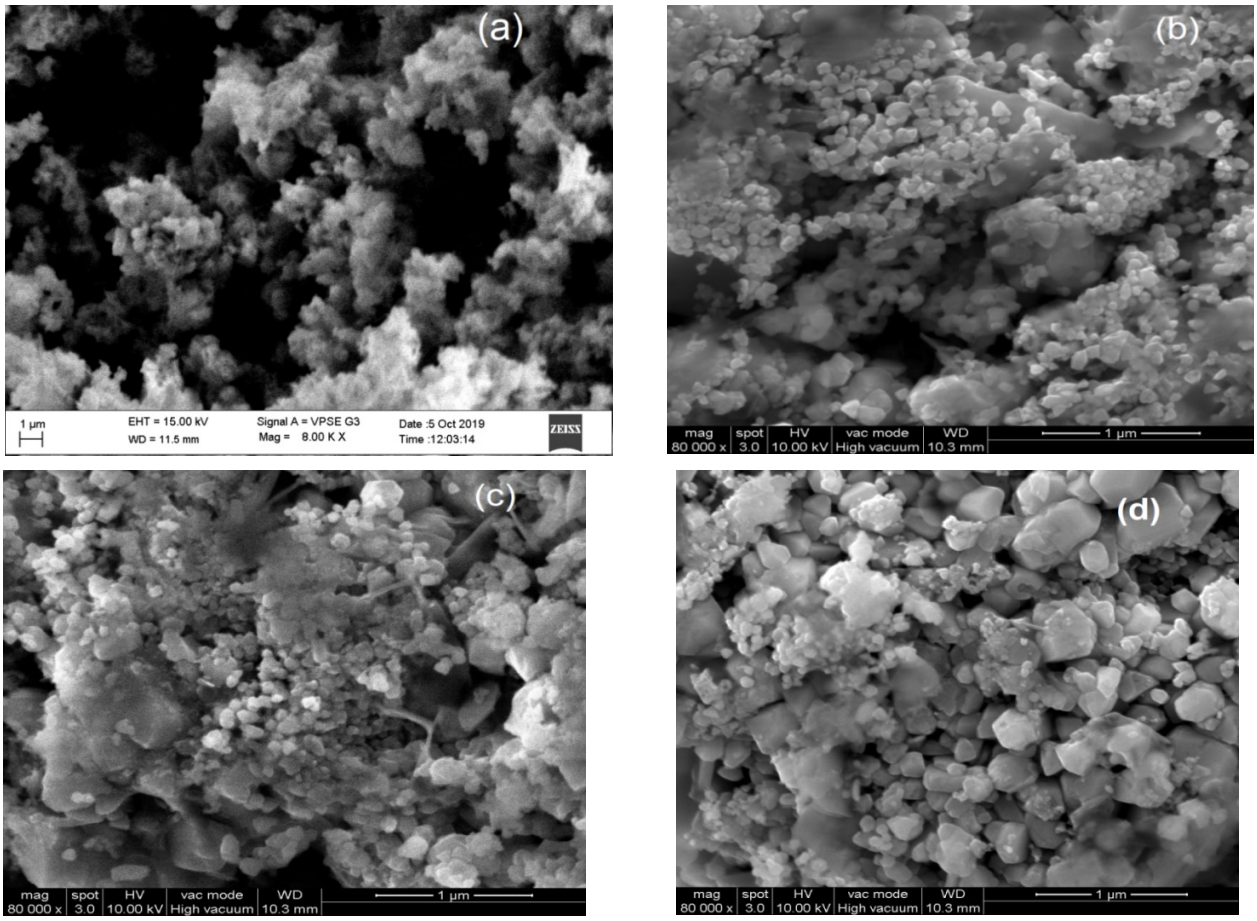

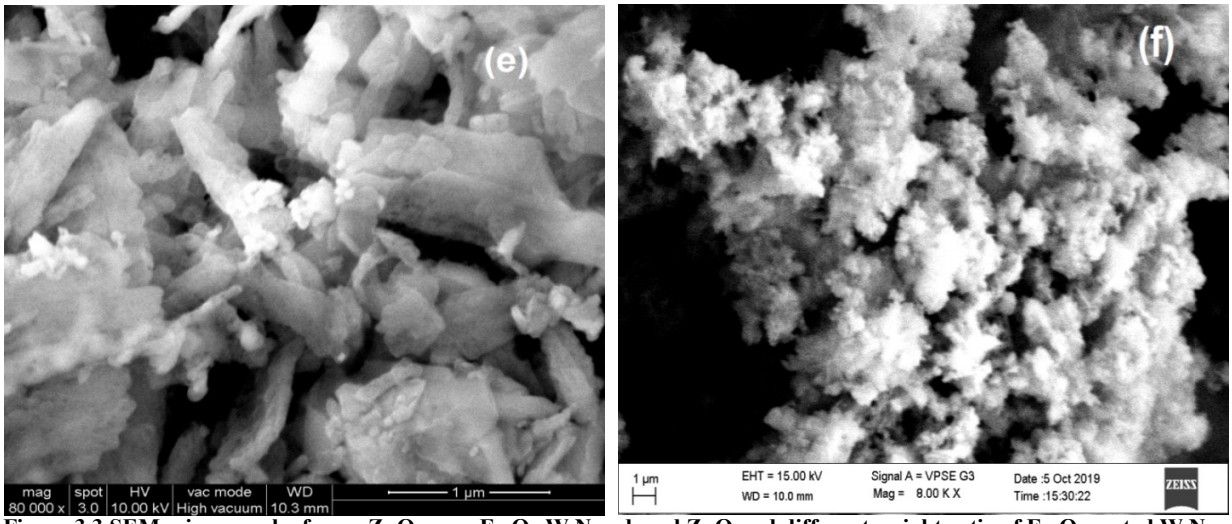

Figure 3.3 SEM micrograph of pure ZnO, pure Fe_2O_3, W,N codoped ZnO and different weight ratio of Fe_2O_3 coated W,N codoped ZnO composites

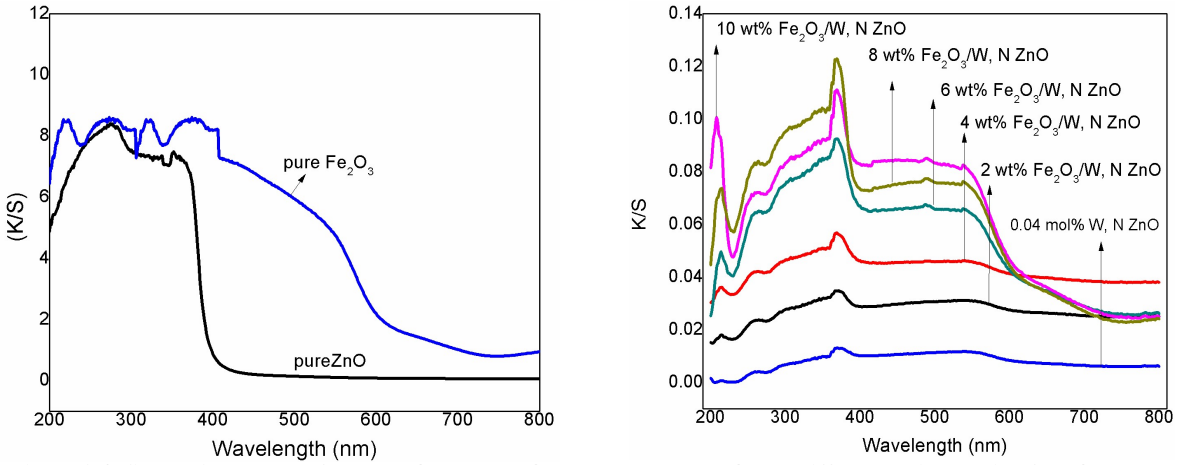

Figure 3.4: SEM micrograph of pure ZnO, pure Fe_2O_3, W,N codoped ZnO and different weight ratio of Fe_2O_3 coated W,N codoped ZnO composites

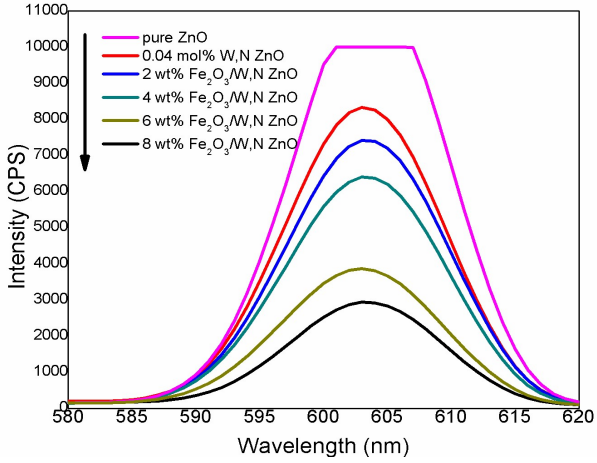

Figure 3.5: photoluminescence (PL) emission spectra of pure ZnO W,N codoped ZnO and Fe_2O_3 coated W, N-codoped ZnO composite photocatalyst

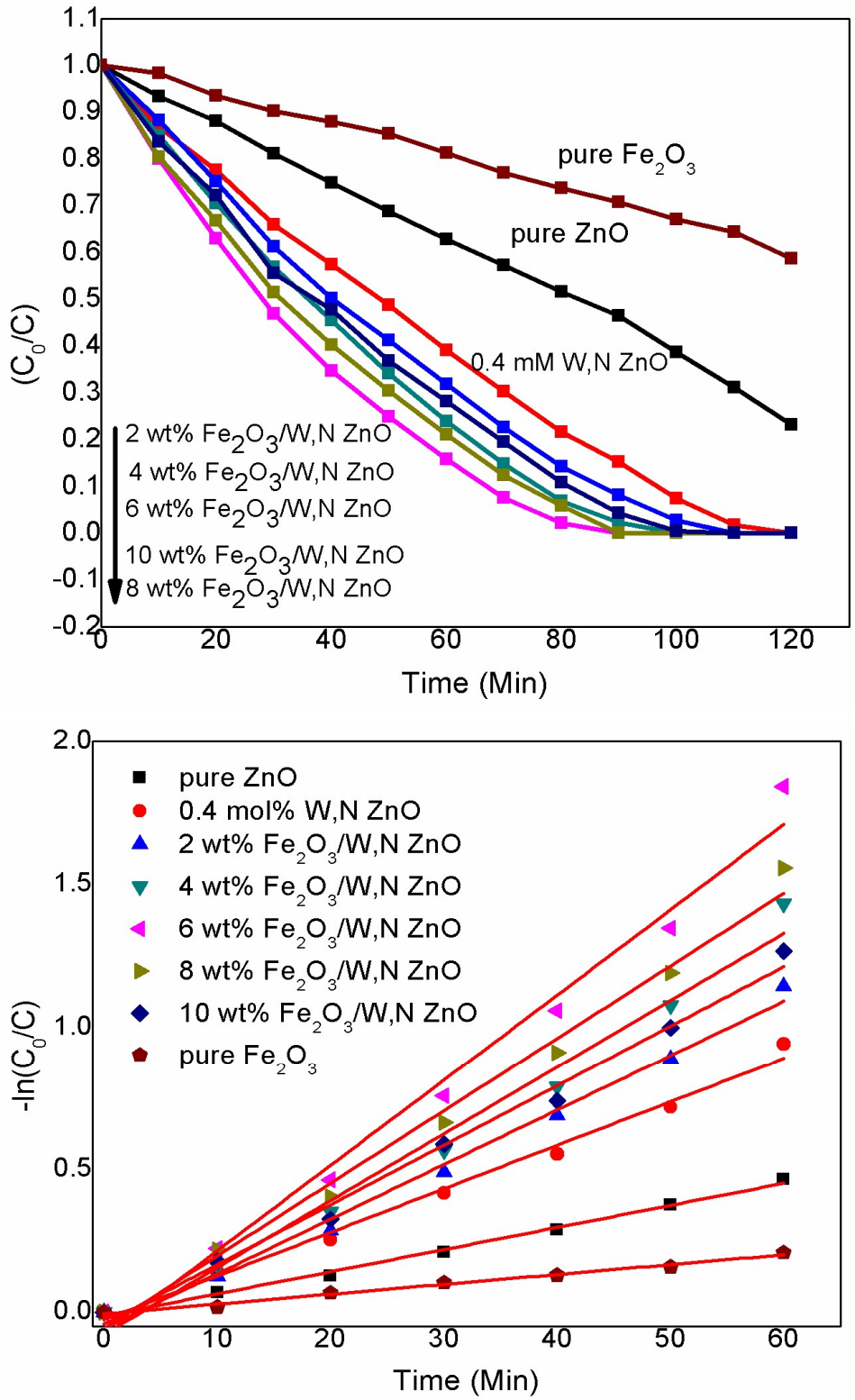

Figure 3.6a: Effect of time on the photocatalytic degradation of dyes; 3.6b: Apparent first order kinetic plots the degradation of Reactive Blue 160.

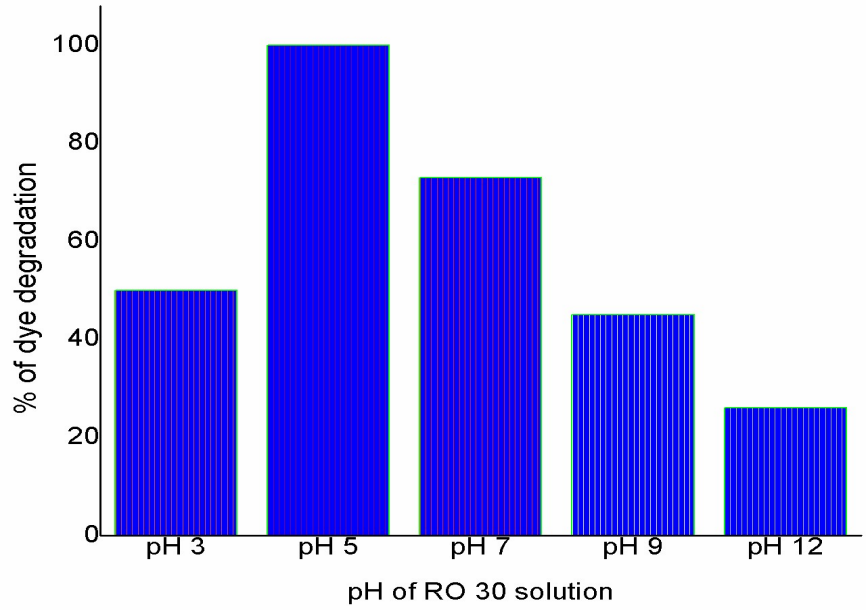

Figure 3.7: Effect of pH on the degradation of RO 30 dye

Table 3.1: COD analysis of the degraded Reactive Blue solution (Irradiation time: 2 hrs)

Photocatalysts	Reactive Blue 160	
	% of degradation	% of reduction in COD
ZnO	100	66
4 wt% Fe_2O_3/ZnO	100	71

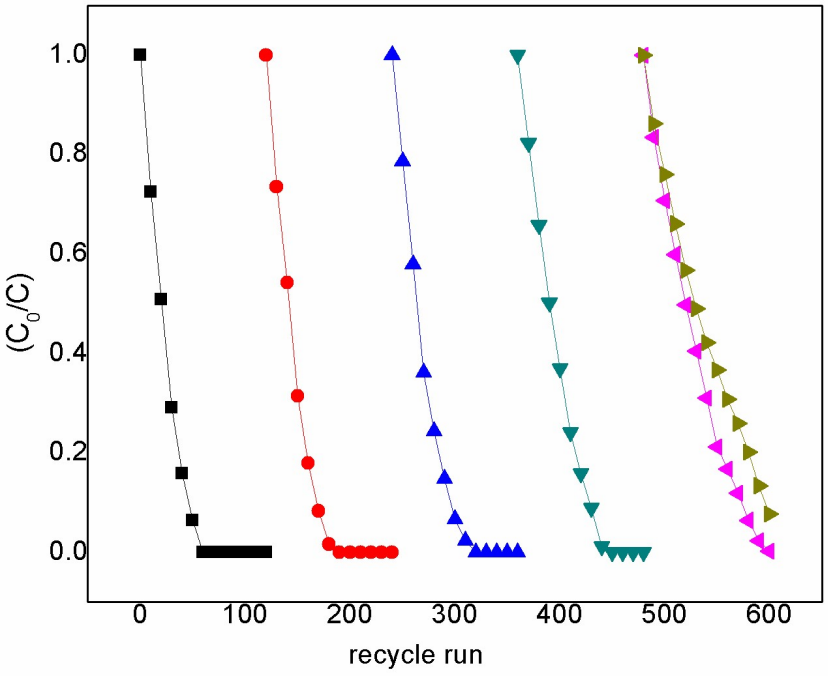

Figure 3.8: Reusability of Fe_2O_3/ W,N codoped ZnO

4. CONCLUSION

Fe_2O_3/ W,N codoped ZnO composites prepared in simple polar solvent despersed method followed by thermal treatment at 300°C for 3 hours has shown good activity for the degradation of RO 30 in solar light. The prepared composite photocatalyst characterized by various techniques and also compared those photocatalytic activities. Fe_2O_3/ W,N codoped ZnO composites has demonstrated highest activity for the degradation of RO 30 a dichloroquinoxaline group and azo group of dye. The rate of degradation of RO 30 over 8 wt% Fe_2O_3/ W,N codoped ZnO composites was maximum when the solution pH was 5. The composite photocatalyst also has good reusability; the 8 wt% Fe_2O_3/ W,N codoped ZnO composites completely degraded RO 30 in 120 minutes even in its fourth reuse. COD analysis of the degraded dye solution shows more than 70% of dye molecules in 50 mg/l reactive dye solution were mineralised in 3 hour of photocatalytic treatment. Hence 4 wt% $CoTiO_3$/Sr, N codoped TiO_2 will be an efficient and cost effective method for the degradation of organic dyes and other organic pollutants in industrial effluent.

REFERENCE

[1] H. Shindy, M. Goma, N. Harb. Novel carbocyanine and biscarbocyanine dyes: synthesis, visible spectra studies, solvatochromism and halochromism, *Chemical Intermediates,* 2, 222–31, 2016.

[2] H. Shindy , A. Khalafalla , M. Goma , A. Eed, Synthesis, photosensitization and antimicrobial activity evaluation of some novel Merocyanine dyes. *Chemical Intermediates* 2, 114–20, 2016.

[3] M. Iqbal , M. Abbas, J. Nisar, A. Nazir, Bioassays based on higher plants as excellent dosimeters for ecotoxicity monitoring: a review. *Chemical Intermediates* 5, 1–80, 2019.

[4] M. Abbas, M. Adil, S. Ehtisham-ul-Haque, B. Munir, M. Yameen, A Ghaffar, et al. Vibrio fischeri bioluminescence inhibition assay for ecotoxicity assessment: a review, *Science of the Total Environment*, 626,1295–309, 2018.

[5] Ghezali S, Mahdad-Benzerdjeb A, Ameri M, Bouyakoub AZ. Adsorption of 2,4,6-trichlorophenol on bentonite modified with benzyldimethyltetradecylammonium chloride. *Chemical Intermediates*, 4, 24–32, 2018.

[6] Mansouri S, Elhammoudi N, Aboul-hrouz S, Mouiya M, Makouki L,

Chham A, et al. Elaboration of novel adsorbent from Moroccan oil shale using Plackett–Burman design. *Chemical Intermediates*, 4, 7–14, 2018.

[7] Alasadi AM, Khaili FI, Awwad AM. Adsorption of Cu(II), Ni(II) and Zn(II) ions by nano kaolinite: thermodynamics and kinetics studies. *Chemical Intermediates* 5, 258–268, 2019.

[8] Qureshi K, Ahmad M, Bhatti I, Iqbal M, Khan A. Cytotoxicity reduction of wastewater treated by advanced oxidation process. *Chemical Intermediates*;1, 53–59, 2015.

[9] Majolagbe AO, Adeyi AA, Osibanjo O. Vulnerability assessment of groundwater pollution in the vicinity of an active dumpsite (Olusosun), Lagos, Nigeria. *Chemical Intermediates*, 2, 232–41, 2016.

[10] Ukpaka C, Ukpaka C. Characteristics of groundwater in Port-Harcourt local government area. *Chemical Intermediates*, 2, 136–44, 2016.

[11] Majolagbe AO, Adeyi AA, Osibanjo O, Adams AO, Ojuri OO. Pollution vulnerability and health risk assessment of groundwater around an engineering landfill in Lagos, Nigeria. *Chemical Intermediates*, 3, 58–68, 2017.

[12] Ajmal S, Bibi I, Majid F, Ata S, Kamran K, Jilani K, et al. Effectof Fe and Bi doping on $LaCoO_3$ structural, magnetic, electric and catalytic properties. *Journal of Material Research and Technology*, 8, 4831–42 2019.

[13] Bibi I, Nazar N, Ata S, Sultan M, Ali A, Abbas A, et al. Green synthesis of iron oxide nanoparticles using pomegranate seeds extract and photocatalytic activity evaluation for the degradation of textile dye, *Journal of Material Research and Technology*, 8, 6115–24, 2019.

[14] Jamil A, Bokhari TH, Javed T, Mustafa R, Sajid M, Noreen S, *et al*. Photocatalytic degradation of disperse dye Violet-26 using TiO2 and ZnO nanomaterials and process variableoptimization. *Journal of Material Research and Technology*, 8, 1119–28, 2019.

[15] Rahmat M, Rehman A, Rahmat S, Bhatti HN, Iqbal M, Khan WS, *et al*. Highly efficient removal of crystal violet dye from water by MnO2 based nanofibrous mesh/photocatalyticprocess. *Journal of*

Material Research and Technology, 8, 5149–59, 2019.

[16] Sohail I, Bhatti IA, Ashar A, Sarim FM, Mohsin M, Naveed R,et al. Polyamidoamine (PAMAM) dendrimers synthesis, characterization and adsorptive removal of nickel ions from aqueous solution. *Journal of Material Research and Technology*, 9, 498–506, 2020.

[17] Zafar MN, Dar Q, Nawaz F, Zafar MN, Iqbal M, Nazar MF. Effective adsorptive removal of azo dyes over spherical ZnO nanoparticles. *Journal of Material Research and Technology*, 8, 713–25, 2019.

[18] Arshad M, Qayyum A, Abbas G, Haider R, Iqbal M, Nazir A.Influence of different solvents on portrayal and photocatalytic activity of tin-doped zinc oxide nanoparticles. Journal of Molecular Liquids, 260, 272–8, 2018.

[19] L. Lin, R.Y. Zheng, J.L. Xie, Y.X. Zhu and Y.C. Xie, Synthesis and characterization of phosphor and nitrogen co-doped titania, *Applied Catalysis B: Environment,* 76, 196–202, 2007.

[20] F. Wei, L. Ni and P. Cui, Preparation and characterization of N-S-codoped TiO_2 photocatalyst and its photocatalytic activity, *Journal of Hazardous Materials* 156, 135-140, 2007.

[21] C. Liu, X. Tang, C. Mo and Z. Qiang, Characterisation and Activity of Visible-Light-Driven TiO_2 Photocatalyst Codoped With Nitrogen and Cerium, *Journal of Solid State Chemistry*, 181, 913–919, 2008.

[22] W. Pingxiao, T. Jianwen and D. Zhi, Preparation and photocatalysis of TiO_2 nanoparticles doped with nitrogen and cadmium, *Material Chemistry and Physics*, 103, 264– 269, 2007.

[23] Wei Xin, Duanwei Zhu, Guanglong Liu, Yumei Hua, and Wenbing Zhou, Synthesis and Characterization of Mn–C–Codoped TiO_2, Nanoparticles and Photocatalytic Degradation of Methyl Orange Dye under Sunlight Irradiation, *International Journal of Photoenergy*, , 17, 2012

[24] R. Khan, S.W. Kim, T-J. Kim and C-M. Nam, Photocatalytic Activity of Toluene under UV-LED Light with TiO_2, *Thin FilmsMaterial Chemistry and Physics*, 112, 167 – 172, 2008.

[25] Qili, josepheaster, N. Jankushang, J. K. As (III) Removal byPalladium-Modified Nitrogen-Doped Titanium

Oxide Nanoparticle Photocatalyst. *Environtal Science and Technology*, 43 (5), 1534 −1539, 2009.

[26] J. Chen, L. Xu, W. Li, X. Gou, α-Fe_2O_3 Nanotubes in Gas Sensor and Lithium-Ion Battery Applications, *Advanced Materials*, 17, 582−586, 2005.

[27] N. Beermann, L. Vayssieres, S. E. Lindquist, A. Hagfeldt, Photoelectrochemical Studies of Oriented Nanorod Thin Films of Hematite, *Journal of Electrochemical Society* 147, 2456−2461, 2000.

[28] Y. W. Zhu, T. Yu, C. H. Sow, Y. J. Liu, A. T. S. Wee, X. J. Xu, C. T. Lim, J. T. L. Thong, *Applied Physics Letters*, 87, 023103− 023105, 2005.

[29] M. A. Valenzuela, P. Bosch, J. Jimenez-Becerril, Quiroz A.I. O, P´aez Preparation, characterization and photocatalytic activity of ZnO, Fe_2O_3 and $ZnFe_2O_4$ *Journal of Photochemistry and Photobiology A: Chemical* 148, 177, 2002.

[30] J. Sene Jeosadeque, W. A Mzeltner, M. A. Anderson Electronic Structure Properties of Carbazole-like Compounds: Implications for Asphaltene Formation, *Journal of Physical Chemistry B* 107, 1597 2003.

[31] K. Chiang, R. Amal, T. Tran Photocatalytic degradation of cyanide using titanium dioxide modified with copper oxide, *Advanced Environmental Research* 6, 471, 2002.

[32] Sadeghi M, Liu W, Zhang T-G, Stavropoulos P, Levy B Directed Photocurrents in Nanostructured TiO_2/SnO_2 Heterojunction Diodes, *Journal of Physics and Chemistry* 100, 19466, 1996.

[33] W. Ho, J.C. Yu, J. Lin, J. Yu, P. Li Preparation and Photocatalytic Behavior of MoS_2 and WS_2 Nanocluster Sensitized TiO_2, *Langmuir* 20, 5865, 2004.

[34] N. Serpone, P. Maruthamuthu, P. Pichat, E. Pelizzetti, H. Hidaka Exploiting the interparticle electron transfer process in the photocatalysed oxidation of phenol, 2-chlorophenol and pentachlorophenol: chemical evidence for electron and hole transfer between coupled semiconductors, *Journal of Photochemistry and Photobiology A: Chemical* 85, 247-255, 1995.

[35] J. Villasenor, P. Reyes, G. Pecchi Photodegradation of pentachlorophenol on ZnO. *Journal of Chemical*

Technology and Biotechnology, 72, 105, 1998.

[36] S.R Pendlebury, M. Barroso, A. J. Cowan, K. Sivula, J. Tang, M. Graetzel, Use of alkyl 2,4,6-triisopropylbenzoates in the asymmetric homologation of challenging boronic esters, *Chemical Communications* 47, 716–718, 2011.

[37] M.M. Mohamed and M.M. Al-Esaimi, Characterization, adsorption and photocatalytic activity of vanadium-doped TiO_2 and sulfated TiO_2 (rutile) catalysts: Degradation of methylene blue dye, *Journal of Molecular Catalysis A: Chemical*, 255, 53, 2006.

[38] B. Naik, K.M. Parida, Solar Light Active Photodegradation of Phenol over a FexTi1−xO_2−yNy Nanophoto-catalyst, *Industrial and Engineering Chemistry Research*, 49 8339-8346, 2010.

[39] S. Liufu, Y. Xiao and H. Li, Investigation of PEG adsorption on the surface of zinc oxide nanoparticles, *Powder Technology* 145, 20–24, 2004.

[40] I.K. Konstantinou, T.A. Albanis, Photocatalytic Transformation of Pesticides in Aqueous Titanium Dioxide Suspensions Using Artificial and Solar Light: Intermediates and Degradation Pathways, *Applied Catalysis B: Environmental* 42, 319-335, 2003

[41] C. Galindo, P. Jacques and A. Kalt, Photochemical and photocatalytic degradation of an indigoid dye: a case study of acid blue 74 (AB74), *Journal of Photochemistry and Photobiology A: Chemical,* 141, 47–56, 2001.